

Inverse mass ordering of light scalar mesons in the Nambu Jona-Lasinio model

Takahiro Saionji¹, Daisuke Jido¹, and Masayasu Harada²

¹*Department of Physics, Tokyo Institute of Technology, Tokyo 152-8551, Japan*

²*Department of Physics, Nagoya University, Nagoya, 464-8602, Japan*

²*Kobayashi-Maskawa Institute for the Origin of Particles and the Universe, Nagoya University, Nagoya, 464-8602, Japan*

²*Advanced Science Research Center, Japan Atomic Energy Agency, Tokai 319-1195, Japan*

.....
The masses of the low-lying scalar mesons are investigated in the three-flavor Nambu Jona-Lasinio (NJL) model by treating the scalar mesons as composite objects of a quark and an antiquark. It is known that a simple $\bar{q}q$ picture fails to reproduce so-called inverse mass ordering for the scalar mesons. Recently a new mechanism to reproduce the observed mass spectrum of the scalar mesons was proposed in a linear sigma model by introducing flavor symmetry breaking induced by the U(1) axial anomaly. Motivated by this proposal, we examine whether this new mechanism works also in the NJL model. By calculating the scalar meson masses, we find that the NJL model reproduces the observed mass ordering with sufficient strength of the new term. With this mechanism, it turns out that the constituent strange quark mass gets degenerate to that of the up and down quark if the inverse mass ordering is reproduced. We also discuss the scalar diquark masses to check the consistency of the degeneracy of the constituent quark masses with the light baryon masses.
.....

Subject Index D32,B60

1. Introduction

The understanding of the structure of the low-lying scalar mesons is important in hadron physics. So far, several scalar mesons have been observed below 1 GeV: $f_0(500)$ with $I = 0$, $K_0^*(700)$ with $I = 1/2$, $f_0(980)$ with $I = 0$ and $a_0(980)$ with $I = 1$ as listed in the particle data table [1]. One of the characteristic feature of these scalar mesons is that, unlike the vector mesons, the mass of the isovector $a_0(980)$ meson is not close to that of the isoscalar $f_0(500)$ meson, and rather the $a_0(980)$ meson being non-strange is heavier than the strange $K_0^*(700)$ meson. It is expected that mesons are composed of a quark and an antiquark. Nevertheless, naive quark models based on the $\bar{q}q$ picture cannot explain the mass ordering of these light scalar mesons, because the masses of hadrons containing strange quarks should be heavier than those without strange quarks there. It has been suggested that this “inverse mass ordering” of the light scalar mesons can be explained by the tetraquark picture $\bar{q}\bar{q}qq$ [2]. In this picture the isovector meson can have a hidden $\bar{s}s$ component and it gives a heavier mass to the meson. Apart from that, these scalar mesons have strong coupling to two pseudoscalar mesons and eventually have a large decay width. Such unstable resonances are described in

hadron-hadron scattering. For instance, the $f_0(500)$ meson can be regarded as a s -wave resonance in the isosinglet pion-pion scattering [3–7]. In these ways, the structure of the scalar mesons being controversial, many pictures for the scalar mesons have been proposed so far such as two-quark $\bar{q}q$, four-quark $\bar{q}\bar{q}qq$, glueball, meson-meson scattering and their mixture [8–22].

Another aspect for the nature of scalar mesons is that there must exist the scalar fields transformed from the pion fields under chiral transformation in quantum chromodynamics (QCD), that is chiral partners of the pions [23]. Chiral symmetry is an approximated symmetry in QCD and is broken dynamically by the flavor-singlet scalar condensate $\langle\bar{q}q\rangle$ with the emergence of the pseudoscalar Nambu-Goldstone bosons corresponding to the pion and its flavor partners. The fluctuation mode of the quark condensate, the σ meson, is regarded as one of the signals for the dynamical breaking of chiral symmetry. It is not understood yet how the sigma meson should appear in the observed spectrum. Here we have the reason that we adhere to the $\bar{q}q$ picture for the scalar mesons.

So far there are several attempts to reproduce the inverse mass ordering in the $\bar{q}q$ picture [9, 24–32]. The key ingredient is the interaction induced by the U(1) axial anomaly [33–41], so-called Kobayashi-Maskawa-’t Hooft (KMT) interaction. For instance, Ref. [28] employed an extended three-flavor Nambu Jona-Lasinio (NJL) model with the six-point KMT interaction to study the mass spectrum of the light scalar mesons. The KMT interaction works for the flavor singlet scalar meson as attractive interaction, while for the octet scalar meson it behaves as repulsive interaction. This term, therefore, contributes to the isosinglet scalar meson to reduce its mass lighter than the other scalar mesons with $I = 1$ and $I = 1/2$. This is consistent with the mass ordering between $f_0(500)$ and the other scalar mesons. The flavor SU(3) breaking is introduced to the NJL model by the mass difference of the current quarks and enters to the meson mass spectrum through the constituent quark masses and the quark condensates. Owing to the flavor singlet nature of the KMT interaction, the KMT interaction works for the strange isodoublet meson with the up or down quark condensate, while it contributes to the isovector meson with the strange quark condensate. Because the absolute value of the strange quark condensate is larger than those of the up and down condensates if the perturbative contributions are included, the repulsion of the KMT interaction is larger for the isovector meson than the isodoublet meson. This is consistent with the inverse mass ordering. Nevertheless, the flavor symmetry breaking in the quark condensates is not so sufficient as to reproduce the inverse ordering of the masses for the $I = 1$ and $I = 1/2$ mesons. Reference [9] was able to reproduce the inverse mass ordering of the light scalar mesons in a linear sigma model with the KMT interaction by introducing unsatisfactorily strong flavor symmetry breaking on the meson decay constants. In an NJL-like model [31, 32], by introducing a large number of terms including explicit flavor symmetry breaking with the current quark mass, the inverse mass ordering was reproduced. Recently Ref. [22] proposed a new mechanism to realize the inverse mass ordering of the scalar mesons in a linear sigma model with a U(1) axial anomaly induced term including the current quark mass. The anomaly induced term with the current quark mass works similarly in the original KMT interaction for the scalar meson masses but with the current quark mass instead of the quark condensate. Thanks to a large flavor symmetry breaking in the current quark masses, say $m_s/m_q \sim 25$, the repulsive anomaly induced interaction contributes to

the isovector meson much more than to the isodoublet meson. Consequently the mass of $a_0(980)$ is provided larger than that of $K_0(700)$ in this model.

In this paper we utilize the Nambu Jona-Lasinio model [42] to study the masses of the light scalar mesons in the $\bar{q}q$ picture. Motivated by Ref. [22] for the linear sigma model, we introduce the chiral anomaly term with the current quark mass to calculate the meson masses. We examine whether this term works to reproduce the inverse mass ordering for the light scalar mesons also in the NJL model.

The paper is organized as follows: In Sect. 2, the formulation of this work is explained. In Sect. 3, we show our numerical results. In Sect. 4 we discuss the diquark masses and the Gell-Mann Oakes Renner relation in this model. Finally Sect. 5 is devoted for the conclusion of this paper. In Appendix calculation details are shown.

2. Nambu Jona-Lasinio model

In order to investigate the masses of the scalar mesons, we consider the Nambu Jona-Lasinio model (NJL model) for the three flavors [43–46]. The Lagrangian that we use here for the quark field $\psi = (u, d, s)^T$ is given as

$$\begin{aligned} \mathcal{L}_{\text{NJL}} = & \bar{\psi}(i\not{\partial} - \mathcal{M})\psi + g_S \sum_{A=0}^8 \left[\left(\bar{\psi} \frac{\lambda_A}{2} \psi \right)^2 + \left(\bar{\psi} i\gamma_5 \frac{\lambda_A}{2} \psi \right)^2 \right] \\ & + \frac{g_D}{2} \{ \det[\bar{\psi}_i(1 + \gamma_5)\psi_j] + \det[\bar{\psi}_i(1 - \gamma_5)\psi_j] \} \\ & + \frac{g_k}{4} \{ \epsilon_{ijk} \epsilon_{abc} \mathcal{M}_{ia} \bar{\psi}_j(1 + \gamma_5)\psi_b \bar{\psi}_k(1 + \gamma_5)\psi_c + (\gamma_5 \rightarrow -\gamma_5) \}, \end{aligned} \quad (1)$$

with the quark mass matrix $\mathcal{M} = \text{diag}(m_q, m_q, m_s)$, the model parameters g_S , g_D , g_k , the Gell-Mann matrices λ^A ($A = 0, 1, \dots, 8$) normalized as $\text{Tr}[\lambda_A \lambda_B] = 2\delta^{AB}$, and the antisymmetric tensor ϵ_{ijk} for $i, j, k = 1, 2, 3$. In this Lagrangian, it is understood that the determinant is taken in the flavor space, the latin letters are the flavor indices of the quark fields running from 1 to 3, and the summations is taken over the repeated indices. We assume isospin symmetry by $m_q = m_u = m_d$. We call the up and down quark fields collectively by q and the strange quark field by s .

The last two terms in Lagrangian (1) are originated from the chiral anomaly in QCD. The term with g_D , known as the Kobayashi Maskawa t'Hooft interaction, provides six-point vertices, and is invariant under the $\text{SU}(3)_L \otimes \text{SU}(3)_R$ but breaks the $\text{U}(1)_A$ symmetry. With the presence of this term the η' meson is degraded from a Nambu Goldstone boson associated with spontaneous breaking of chiral symmetry. The term containing g_k is also an anomalous interaction and provides four-point interactions of quarks. It breaks chiral symmetry explicitly with the quark mass term \mathcal{M} and the flavor symmetry is also broken by the quark mass difference $m_q \neq m_s$. This term is uniquely determined by the $\text{U}(1)_A$ anomaly and the $\text{SU}(3)$ flavor symmetry with one quark mass term \mathcal{M} . This type of interactions was introduced into a linear sigma model in Ref. [22] to investigate the inverse mass hierarchy of the scalar mesons and is also found in Ref. [31] as L_2 for the NJL-like model. Because containing the totally antisymmetric tensor ϵ_{ijk} in the flavor space, this term contributes to non-strange systems with the strange quark mass and to systems having the strange quarks with the light quark mass. Therefore, the term provides significantly stronger interactions for the non-strange systems.

Employing the mean field approximation [46] by replacing the quark fields in the Lagrangian as

$$\bar{\psi}_i \psi_i \bar{\psi}_j \psi_j \rightarrow \langle \bar{\psi}_i \psi_i \rangle \bar{\psi}_j \psi_j + \langle \bar{\psi}_j \psi_j \rangle \bar{\psi}_i \psi_i - \langle \bar{\psi}_i \psi_i \rangle \langle \bar{\psi}_j \psi_j \rangle, \quad (2)$$

$$\begin{aligned} \bar{\psi}_i \psi_i \bar{\psi}_j \psi_j \bar{\psi}_k \psi_k &\rightarrow \langle \bar{\psi}_i \psi_i \rangle \langle \bar{\psi}_j \psi_j \rangle \bar{\psi}_k \psi_k + \langle \bar{\psi}_k \psi_k \rangle \langle \bar{\psi}_i \psi_i \rangle \bar{\psi}_j \psi_j + \langle \bar{\psi}_j \psi_j \rangle \langle \bar{\psi}_k \psi_k \rangle \bar{\psi}_i \psi_i \\ &\quad - 2 \langle \bar{\psi}_i \psi_i \rangle \langle \bar{\psi}_j \psi_j \rangle \langle \bar{\psi}_k \psi_k \rangle, \end{aligned} \quad (3)$$

where ψ_i ($i = 1, 2, 3$) is either u , d or s quark field and the summation is not taken for the repeated indices, we obtain the gap equations for the dynamical masses of the light and strange quarks, M_q and M_s , as

$$M_q = m_q - g_S \langle \bar{q}q \rangle - g_D \langle \bar{q}q \rangle \langle \bar{s}s \rangle - g_k (m_q \langle \bar{s}s \rangle + m_s \langle \bar{q}q \rangle), \quad (4a)$$

$$M_s = m_s - g_S \langle \bar{s}s \rangle - g_D \langle \bar{q}q \rangle^2 - 2g_k m_q \langle \bar{q}q \rangle, \quad (4b)$$

with the isospin symmetry $\langle \bar{q}q \rangle = \langle \bar{u}u \rangle = \langle \bar{d}d \rangle$.

We evaluate the quark condensate from the quark propagator $S_F(x) = -i \langle 0 | T[\psi(x) \bar{\psi}(x)] | 0 \rangle$ with the dynamical mass M as

$$\langle \bar{\psi}\psi \rangle = -i N_c \lim_{x \rightarrow 0} \text{Tr}[S_F(x)] = -i N_c \int \frac{d^4 q}{(2\pi)^4} \text{Tr} \left[\frac{1}{\not{p} - M + i\epsilon} \right], \quad (5)$$

where N_c is the number of color, that is $N_c = 3$, and Tr is taken for the Dirac indices. To regularize the momentum integral, we make use of the three-momentum cutoff Λ in accordance with the suggestion given in Ref. [46]. The calculated result of Eq. (5) is given in Eq. (A1). In the present work, the cutoff Λ , which determines the mass scale of the scalar meson, is to be fixed at $\Lambda = 650$ MeV commonly for three quarks. The qualitative consequences do not change in a small change of the value of the cutoff and the corresponding adjustment of the model parameters. With sufficiently large couplings in magnitude, the gap equations (4) provide nontrivial solutions where chiral symmetry is dynamically broken. We introduce dimensionless coupling constants as

$$G_S = \frac{g_S}{g_S^0}, \quad G_D = \frac{\Lambda g_D}{(g_S^0)^2}, \quad G_k = \frac{\Lambda g_k}{g_S^0}, \quad (6)$$

with

$$g_S^0 = \frac{2\pi^2}{3\Lambda^2}, \quad (7)$$

which is the critical coupling of the dynamical symmetry breaking for $g_D = g_k = 0$ in the chiral limit.

In order to calculate the meson masses, let us consider the quark-antiquark scattering amplitude T , which is defined as

$$T(P) = \int d^4 x \langle 0 | T \Phi(x) \Phi(0) | 0 \rangle e^{-iP \cdot x}, \quad (8)$$

where $\Phi(x)$ is an interpolating field of the meson of interest and is given by $\Phi(x) = \bar{\psi}_i \psi_j$ for the scalar meson and $\Phi(x) = \bar{\psi}_i i \gamma_5 \psi_j$ for the pseudoscalar meson. The quark indices i, j stand for the flavor of the quark and are appropriately chosen to provide the meson flavor. For the isospin $I = 0$ configurations of the flavor singlet and octet, we consider their quark contents to be $\Phi_0 = \frac{1}{\sqrt{3}}(\bar{u}u + \bar{d}d + \bar{s}s)$ and $\Phi_8 = \frac{1}{\sqrt{6}}(\bar{u}u + \bar{d}d - 2\bar{s}s)$, respectively. The

Scalar mesons	
$\Phi_{a_0} = \bar{q} \frac{\tau^a}{\sqrt{2}} q,$	$\Phi_\kappa = \bar{s} q,$
$\Phi_8^S = \frac{1}{\sqrt{6}}(\bar{u}u + \bar{d}d - 2\bar{s}s),$	$\Phi_0^S = \frac{1}{\sqrt{3}}(\bar{u}u + \bar{d}d + \bar{s}s),$
Pseudoscalar mesons	
$\Phi_\pi = \bar{q} i \gamma_5 \frac{\tau^a}{\sqrt{2}} q,$	$\Phi_K = \bar{s} i \gamma_5 q,$
$\Phi_8^P = \frac{1}{\sqrt{6}}(\bar{u} i \gamma_5 u + \bar{d} i \gamma_5 d - 2\bar{s} i \gamma_5 s),$	$\Phi_0^P = \frac{1}{\sqrt{3}}(\bar{u} i \gamma_5 u + \bar{d} i \gamma_5 d + \bar{s} i \gamma_5 s),$

Table 1 Quark contents of the meson interpolating fields. q is the isodoublet quark field and τ^a is the Pauli matrix for the isospin space.

explicit quark contents of the interpolating fields are summarized in Table 1. Here we call the isodoublet scalar meson κ and the isovector scalar meson a_0 .

The mesons are dynamically generated in quark-antiquark scattering with sufficiently strong attraction between the quark and the antiquark, and are expressed as poles of the scattering amplitude T . We calculate the T -matrix by solving the Bethe-Salpeter equation:

$$T = K + KJT, \quad (9)$$

with the interaction kernel K and the quark loop function J . Here we use the ladder approximation in the center of mass frame.

The interaction kernel K is obtained directly from the four-point interactions of the g_S and g_k terms in Lagrangian (1) and also from the six-point interaction with the mean field approximation. The explicit form of each channel is given as

$$K_{a_0} = g_S - g_D \langle \bar{s}s \rangle - g_k m_s, \quad (10a)$$

$$K_\kappa = g_S - g_D \langle \bar{q}q \rangle - g_k m_q, \quad (10b)$$

$$K_{00}^S = g_S + \frac{2}{3}g_D(2\langle \bar{q}q \rangle + \langle \bar{s}s \rangle) + \frac{2}{3}g_k(2m_q + m_s), \quad (10c)$$

$$K_{88}^S = g_S - \frac{1}{3}g_D(4\langle \bar{q}q \rangle - \langle \bar{s}s \rangle) - \frac{1}{3}g_k(4m_q - m_s), \quad (10d)$$

$$K_{08}^S = -\frac{\sqrt{2}}{3}g_D(\langle \bar{q}q \rangle - \langle \bar{s}s \rangle) - \frac{\sqrt{2}}{3}g_k(m_q - m_s), \quad (10e)$$

for the scalar mesons and

$$K_\pi = g_S + g_D \langle \bar{s}s \rangle + g_k m_s, \quad (11a)$$

$$K_K = g_S + g_D \langle \bar{q}q \rangle + g_k m_q, \quad (11b)$$

$$K_{00}^P = g_S - \frac{2}{3}g_D(2\langle \bar{q}q \rangle + \langle \bar{s}s \rangle) - \frac{2}{3}g_k(2m_q + m_s), \quad (11c)$$

$$K_{88}^P = g_S + \frac{1}{3}g_D(4\langle \bar{q}q \rangle - \langle \bar{s}s \rangle) + \frac{1}{3}g_k(4m_q - m_s), \quad (11d)$$

$$K_{08}^P = \frac{\sqrt{2}}{3}g_D(\langle \bar{q}q \rangle - \langle \bar{s}s \rangle) + \frac{\sqrt{2}}{3}g_k(m_q - m_s), \quad (11e)$$

for the pseudoscalar mesons. Thanks to the flavor symmetry breaking, $m_q \neq m_s$ and $\langle \bar{q}q \rangle \neq \langle \bar{s}s \rangle$, we have the mixing between the flavor singlet and octet for $I = 0$.

The loop function J is defined with $P^\mu = (W, 0, 0, 0)$ by

$$J_S(W; M_1, M_2) = N_c i \int \frac{d^4 p}{(2\pi)^4} \text{Tr} \left[\frac{1}{\not{p} - M_1 + i\epsilon} \frac{1}{\not{p} - \not{P} - M_2 + i\epsilon} \right], \quad (12)$$

for the scalar channel and

$$J_P(W; M_1, M_2) = N_c i \int \frac{d^4 p}{(2\pi)^4} \text{Tr} \left[i\gamma_5 \frac{1}{\not{p} - M_1 + i\epsilon} i\gamma_5 \frac{1}{\not{p} - \not{P} - M_2 + i\epsilon} \right], \quad (13)$$

for the pseudoscalar channel. We calculate the loop function with the same three momentum cutoff Λ as the calculation of the quark condensate. This procedure keeps chiral symmetry in the calculation. The explicit forms of the loop functions are shown in Eqs. (A2) for the scalar channel and (A3) for the pseudoscalar channel. The loop function for each meson channel is listed as

$$J_{a_0/\pi}(W) = J_{S/P}(W; M_q, M_q), \quad (14a)$$

$$J_{\kappa/K}(W) = J_{S/P}(W; M_q, M_s), \quad (14b)$$

$$J_{00}^{S/P}(W) = \frac{1}{3}(2J_{S/P}(W; M_q, M_q) + J_{S/P}(W; M_s, M_s)), \quad (14c)$$

$$J_{88}^{S/P}(W) = \frac{1}{3}(J_{S/P}(W; M_q, M_q) + 2J_{S/P}(W; M_s, M_s)), \quad (14d)$$

$$J_{08}^{S/P}(W) = \frac{\sqrt{2}}{3}(J_{S/P}(W; M_q, M_q) - J_{S/P}(W; M_s, M_s)). \quad (14e)$$

The meson mass is obtained as the pole position of the scattering amplitude $T(W)$. In the ladder approximation the Bethe-Salpeter equation (9) can be solved in an algebraic way as

$$T(W) = \frac{1}{1 - KJ(W)}K. \quad (15)$$

We find the pole position of the scattering amplitude T by solving

$$1 - KJ(W) = 0, \quad (16)$$

for the single channel case. The loop function $J(W)$ in the complex W plane has two Riemann sheets corresponding to the sign of the momentum and the branch cut runs along the real axis from the threshold of the particle production $W = M_1 + M_2$ to $+\infty$. The solutions of Eq. (16) found in the first Riemann sheet and below the threshold correspond to the bound states. The bound state solutions appear on the real axis. On the other hand, solutions found in the second Riemann sheet correspond to virtual or resonance states; the virtual states are found below the threshold, while the resonance states are above the threshold. Because of the lack of the confinement mechanism in the NJL model the mesons that are generated above the threshold have a decay to fall apart into the quark and the antiquark. These decays are indeed model artifacts of the NJL model.

With the flavor symmetry breaking, the $I = 0$ channels of the flavor singlet and octet couple each other and the Bethe-Salpeter equation becomes a matrix equation:

$$\begin{pmatrix} T_{00} & T_{08} \\ T_{08} & T_{88} \end{pmatrix} = \begin{pmatrix} K_{00} & K_{08} \\ K_{08} & K_{88} \end{pmatrix} + \begin{pmatrix} K_{00} & K_{08} \\ K_{08} & K_{88} \end{pmatrix} \begin{pmatrix} J_{00} & J_{08} \\ J_{08} & J_{88} \end{pmatrix} \begin{pmatrix} T_{00} & T_{08} \\ T_{08} & T_{88} \end{pmatrix}. \quad (17)$$

The pole positions of the T -matrix are obtained for the coupled-channels case by

$$\det(1 - KJ(W)) = 0. \quad (18)$$

m_π	m_K	$m_{\eta'}$	f_π
138.04	495.65	957.78	92.2

Table 2 Input parameters in units of MeV.

G_k	0.0	0.5	1.0	1.5	2.0	PDG [1]
m_q [MeV]	5.32	4.35	3.74	3.31	2.99	$3.45^{+0.35}_{-0.15}$
m_s [MeV]	134.79	115.73	101.39	90.24	81.34	$93.4^{+8.6}_{-3.4}$
G_S	0.870	0.845	0.826	0.812	0.800	—
G_D	-0.865	-0.768	-0.692	-0.630	-0.579	—
m_s/m_q	25.35	26.60	27.15	27.28	27.17	$27.33^{+0.67}_{-0.77}$

Table 3 Determined parameters for $G_k = 0.0, 0.5, 1.0, 1.5$ and 2.0 . The last column shows the values for current quark masses picked up from the Review of Particle Physics (2022) [1]. The dimensionless interaction parameters, G_S , G_D and G_k , are defined in Eq. (6). The cutoff is fixed as $\Lambda = 650$ MeV.

We call the energetically lower solution for the scalar (pseudoscalar) meson by σ (η), while the higher solution denotes σ' (η').

The decay constant F for the pseudoscalar meson Φ^a is defined by

$$\langle 0 | A_\mu^a(x) | \Phi^b(P) \rangle = i \delta^{ab} P_\mu F e^{-iP \cdot x}, \quad (19)$$

with the axial vector current $A_\mu^a = \bar{\psi} \gamma_\mu \gamma_5 \frac{\lambda^a}{2} \psi$, and calculated in the current NJL model as

$$F = -i \sqrt{2R} J_A(m), \quad (20)$$

with the meson mass m and the residue R of the T matrix (8) as a function of W^2 at $W^2 = m^2$. The loop function J_A with the axial current is defined by

$$P^\mu J_A(W; M_1, M_2) \equiv i N_c \int \frac{d^4 p}{(2\pi)^4} \text{Tr} \left[\frac{\gamma^\mu \gamma_5}{2} \frac{1}{\not{p} - M_1 + i\epsilon} i \gamma_5 \frac{1}{\not{p} - \not{P} - M_2 + i\epsilon} \right]. \quad (21)$$

The loop function J_A is also calculated with the same three-momentum cutoff Λ as Eq. (5). The explicit form is shown in Eq. (A8) in appendix.

3. Results

In this section, we show our calculated results. In Sect. 3.1 we discuss the determined parameters. In Sect. 3.2 we show our numerical results for the scalar meson masses. In Sect. 3.3 we discuss the constituent quark masses for finite G_k .

3.1. Determined parameters

The model parameters, m_q , m_s , G_S and G_D , are determined for each G_k so as to reproduce the masses of π , K and η' and the pion decay constant. The explicit values of these input quantities are shown in Table 2. Since the η' meson in this model is found as a resonance with a large width above the threshold of the strange quark-antiquark production, we reproduce the observed η' mass by the real part of the calculated resonance mass.

G_k		0.0	0.5	1.0	1.5	2.0
$\text{Re}(m_{a_0})$	[MeV]	844	865	883	898	912
$\text{Re}(m_\kappa)$	[MeV]	970	923	886	857	832
m_σ	[MeV]	585	584	583	582	581
$\text{Re}(m_{\sigma'})$	[MeV]	1077	991	925	873	832
m_η	[MeV]	533	552	560	559	554
M_q	[MeV]	309	309	309	309	309
M_s	[MeV]	475	428	392	362	338
$(-\langle\bar{q}q\rangle)^{1/3}$	[MeV]	248	248	248	248	248
$(-\langle\bar{s}s\rangle)^{1/3}$	[MeV]	269	265	261	257	253
f_K	[MeV]	98	96	95	94	92

Table 4 Results of the physical quantities obtained in the present calculation. The cutoff is fixed as $\Lambda = 650$ MeV.

The determined model parameters for $G_k = 0.0, 0.5, 1.0, 1.5$ and 2.0 are shown in Table 3. We find that the values of the current quark masses m_q and m_s and their ratio for $G_k = 2.0$ are more consistent with the values given in the Review of Particle Physics (2022) [1] than those for $G_k = 0.0$. In Table 3 we also find that the sizes of all the model parameters get smaller for larger G_k . In particular, the current strange quark mass m_s and the magnitude of G_D are more strongly reduced. These behaviors can be explained by the following argument. We determine the model parameters so as to reproduce the observed masses of pion and kaon. The meson masses are obtained as the pole position of the T -matrix, which is calculated by the Bethe-Salpeter equation (9) with the interaction kernel K . To keep the pion mass as the G_k increases, the interaction kernel for pion should also stay as it is for $G_k = 0$. According to Eq. (11a), as the effect of the G_k term increases with a massive m_s , the effects of the G_S and G_D terms should be reduced, and thus, the sizes of G_S and G_D have to decrease. Note in Eq. (11a) that both G_D and $\langle\bar{s}s\rangle$ have a negative value. Because the G_k term comes with a small m_q for kaon in Eq. (11b), its effect is insignificant for the interaction kernel for kaon. This would make K_K reduced and the kaon channel would get more repulsive. To keep the kaon mass in this repulsive change, the current strange quark mass should be reduced.

It is also interesting to mention that G_S is less than unity. According to Ref. [47], this situation is called anomaly-driven symmetry breaking, where the $U(1)_A$ anomaly plays an essential role for the dynamical breaking of chiral symmetry. In such a situation, the mass of the sigma meson should be smaller than 800 MeV. The current model also suggests that the anomaly-driven symmetry breaking takes place and predicts that the sigma meson mass is found to be less than 800 MeV as we will show in the next subsection.

3.2. Scalar meson masses

Fixing the model parameters for each G_k , we calculate the meson masses for G_k from 0.0 to 2.0. The results are summarized in Table 4. The σ and η mesons are found below the threshold of the $\bar{q}q$ pair creation without a decay width. This implies that they are bound states of two constituent quarks and do not decay into the quark pair nor mesonic modes. This is because we do not consider mesonic decay channels in the Bethe-Salpeter equations.

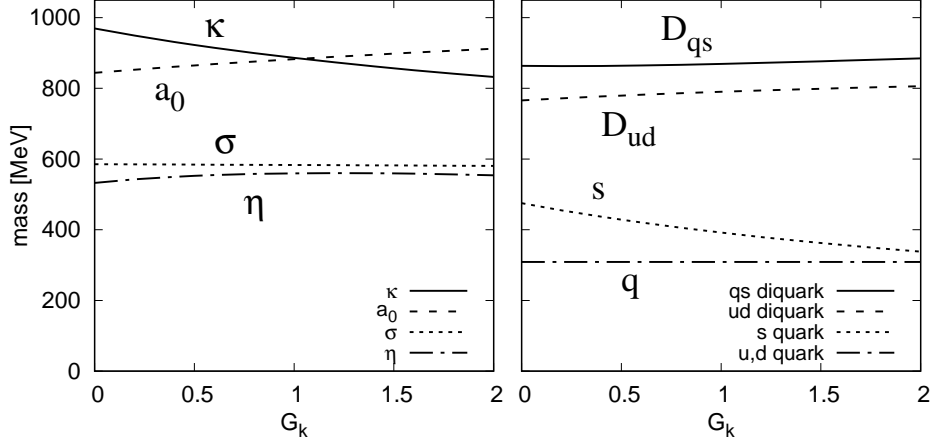


Fig. 1 Dependence of the masses of the mesons, the constituent quarks and the diquarks to the G_k parameter. The left panel shows the meson masses, while the right plots the masses of the constituent quark and the diquarks. For discussion on the diquark masses, see Sect. 4.1. The real parts of the resonance masses are plotted. The cutoff is fixed as $\Lambda = 650$ MeV.

On the other hand, the a_0 , κ and σ' mesons are found as resonances with decay widths. The a_0 and κ mesons are generated in the single \bar{q} - q and \bar{s} - q scattering channels, respectively, and these resonance states are located above the thresholds of these channels. The σ' mesons are in the coupled channels of the \bar{q} - q and \bar{s} - s scatterings and are found above both thresholds. The decay widths of these mesons are far apart of the quark and antiquark due to the lack of the confinement mechanism in the NJL model. Therefore these decay widths are model artifacts and we do not discuss their details. For this reason, in Table 4 we show only the real parts of the meson masses. In Table 4 we show also our calculated results of the constituent quark masses, M_q and M_s , the quark condensates, $\langle \bar{q}q \rangle$ and $\langle \bar{s}s \rangle$, and the kaon decay constant f_K .

Let us first discuss the case of $G_k = 0.0$, which is the original NJL model with the determinant interaction. The constituent quark masses, M_q and M_s , are found as 309 MeV and 475 MeV, respectively, which are consistent with the empirical values. The kaon decay constant is underestimated in the present calculation, but this is known as one of the drawbacks of the NJL model [48]. As mentioned in introduction, thanks to the heavy strange quark mass than those of the up and down quarks, the mass of the κ meson is heavier than that of the a_0 meson, which is the normal mass ordering and inconsistent with the observation. The σ meson is reproduced with a 600 MeV mass, which is consistent with an empirical value. The η meson mass is reproduced reasonably well, although it is a bit underestimated in comparison with the observed η meson mass.

We plot the G_k dependence of the meson masses in the left panel of Fig. 1. This figure shows that, as the value of G_k increases, the mass of the κ meson decreases while the a_0 mass increases. It is remarkable that at $G_k \sim 1$ the mass of the κ meson becomes lighter than that of the a_0 meson. Thus, the inverse mass order of the κ and a_0 mesons is realized for $G_k > 1.0$. This is understood as follows. We show the G_k dependence of the interaction kernels in Fig. 2. As seen in the left panel, the interaction kernel of the a_0 meson decreases as

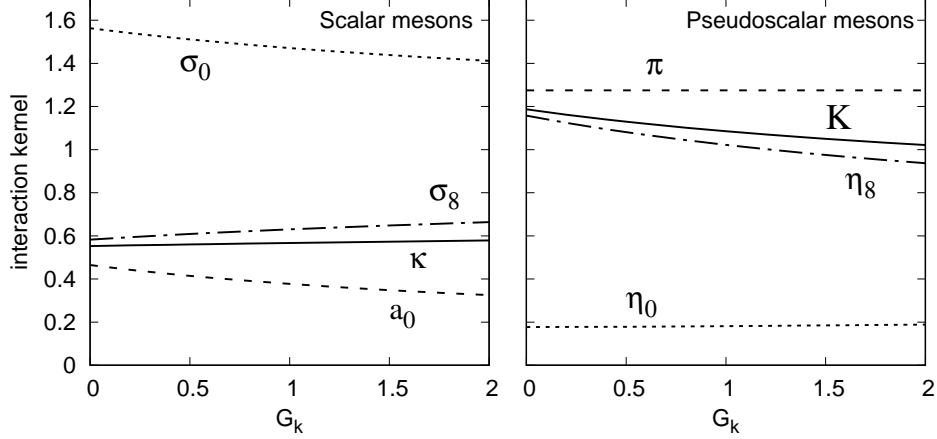


Fig. 2 Dependence of the determined interaction kernels in units of $g_S^0 \equiv 2\pi^2/(3\Lambda^2)$ to the G_k parameter. The left panel is for the scalar meson, while the right for the pseudoscalar mesons. The interaction kernel for each meson is given in Eq. (10) for the scalar mesons and Eq. (11) for the pseudoscalar mesons.

state	componet	$G_k = 0.0$	$G_k = 1.0$	$G_k = 2.0$
σ	singlet	97.2 %	96.5 %	96.3 %
	octet	2.8 %	3.5 %	3.7 %
σ'	singlet	22.0 %	11.3 %	5.1 %
	octet	78.0 %	88.7 %	94.9 %
η'	singlet	98.8 %	98.5 %	97.5 %
	octet	1.2 %	1.5 %	2.5 %
η	singlet	0.0 %	0.7 %	2.1 %
	octet	100.0 %	99.3 %	97.9 %

Table 5 Obtained flavor contents of the σ , σ' , η and η' mesons for $G_k = 0.0, 1.0$ and 2.0 .

G_k increases on one hand. This is because, as seen in Eq. (10a), the negative contribution of the G_k term to the interaction kernel K_{a_0} appears with a large current mass of the strange quark. On the other hand, the interaction kernel for the κ meson increases gradually. This is because, for the κ meson, the G_k term comes with the small current quark mass m_q and its contribution gets minor for the interaction kernel K_κ . In this way, we confirm that the new mechanism proposed in Ref. [22] works well also in the NJL model.

Figure 1 shows that the σ meson mass gradually decreases as G_k increases. One may wonder why the σ meson mass decreases although the interaction kernel for the σ meson gets weaker as seen in Fig. 2. This is because in the σ meson the flavor singlet component is dominated as shown in Table 5, and thus the strange quark is also one of the main components of the σ meson. In addition, as seen in Fig. 1, the constituent strange quark mass gets reduced as G_k increases, which will be discussed in the next section. Because the mass of the constituents gets reduced, the mass of the σ meson decreases even though the coupling strength gets weaker.

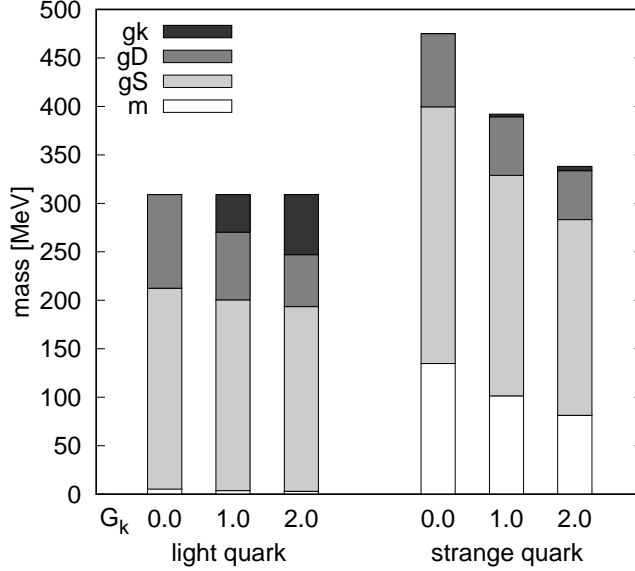


Fig. 3 Contents of the constituent quark masses for $G_k = 0.0, 1.0, 2.0$. The constituent quark masses are decomposed accordingly to the right hand sides of the gap equations (4). Symbols in the key, m , gS , gD and gk , stand for the contributions from the first, second, third and fourth terms of the right hand sides of Eq. (4), respectively.

3.3. Constituent quark masses

It is also interesting noting that Fig. 1 shows that the constituent strange quark also reduces its mass M_s as the G_k increases, while the constituent quark mass M_q stays at the same value. This is also one of the reasons that the κ meson mass is reduced with the increase of G_k . In order to understand the origin of the reduction of the strange quark mass, let us decompose the contents of the constituent quark masses. The constituent quark masses are determined by the gap equations (4). The quark masses can be decomposed accordingly to the right hand side of Eq. (4), and we show this decomposition of the quark masses in Fig. 3. For the light quarks, u and d , one finds that the contribution of the G_k term is enhanced for larger G_k . This is because the G_k term for the light quarks appears with the current strange quark mass m_s . At the same time, the contributions from the G_S and G_D terms get reduced. The contribution from the current quark mass is negligibly small for the light quarks. For the strange quark, the contribution of the G_k term is negligible, because this term appears together with the tiny current quark mass m_q in the gap equation for the strange quark mass. Therefore, for the strange quark, there is no enhanced contributions for larger G_k . In addition, the contribution from the current quark mass gets also smaller with the reduction of the current strange quark mass.

4. Discussion

4.1. Diquark mass

With a finite G_k we obtain a smaller constituent strange quark mass. For $G_k \simeq 2.0$ where the inverse mass ordering is realized, the constituent strange quark gets almost degenerate to the constituent up-down quark. This means that the SU(3) breaking on the constituent quark

Scalar diquarks
$\Phi_{ud}^a = \frac{\epsilon_{abc}}{\sqrt{2}}(u_b^T C \gamma_5 d_c - d_b^T C \gamma_5 u_c),$
$\Phi_{qs}^a = \frac{\epsilon_{abc}}{\sqrt{2}}(q_b^T C \gamma_5 s_c - q_s^T C \gamma_5 s_c),$

Table 6 Quark contents of the diquark interpolating fields. Indices a, b, c are for the color space, q is the isodoublet quark field and C is the charge conjugation matrix.

masses gets weaker. In such a situation, one may wonder whether this degeneracy of the constituent quarks would be inconsistent with the baryon mass spectra, where substantial SU(3) flavor breaking is present. Here, instead of calculating the baryon masses directly in Faddeev approaches developed in Refs. [49–53], rather we calculate the diquark masses, because the diquarks are significant ingredients of the baryons and the baryon masses can be expressed in terms of the diquark mass together with the constituent quark mass [54–56].

We consider flavor-antisymmetric scalar diquarks, so-called good diquarks, which are the most attractive channels among the diquarks. The interpolating fields for the scalar diquarks are shown in Table 6. To obtain the scalar diquark masses, we calculate the pole position of the scattering matrix of the two quark system using the Bethe-Salpeter equation (9). The interaction kernels for the diquark channels are also obtained from Lagrangian (1) by performing a Fierz transformation. But it is known that the Fierz transform of the g_S term in Lagrangian (1) does not provides the scalar diquark interactions. Here we assume that the strength of the g_S term for the scalar diquark channels is a quarter of that of the pseudoscalar meson channel, which is obtained in the Fierz transformation of the color current interaction $\mathcal{L}_{\text{int}} = -G_c \sum_{a=1}^8 (\bar{\psi} \gamma_\mu t^a \psi)^2$, where t^a is the generator of color space. It is our aim to see the dependence of the diquark mass to the G_k parameter, while we are not interested in the quantitative reproduction of the diquark masses. Thus, the exact value of the coefficient of the g_S term is irrelevant to our discussion. The g_D and g_k terms for the diquark channels can be obtained by the Fierz transformation of Lagrangian (1), and then we have the interaction kernel of the diquark channels as

$$K_{ud} = \frac{1}{4}g_S + \frac{1}{2}g_D \langle \bar{s}s \rangle + \frac{1}{4}g_k m_s, \quad (22a)$$

$$K_{qs} = \frac{1}{4}g_S + \frac{1}{2}g_D \langle \bar{q}q \rangle + \frac{1}{4}g_k m_q. \quad (22b)$$

The loop function for the diquark channel is defined by the correlation of the interpolating fields $\Phi_D^a(x)$ given in Table 6 with (anti)color a and is obtained as the same form as the loop function for the pseudoscalar meson channel:

$$J_D^{ab}(W) = i \int d^4x e^{iP \cdot x} \langle 0 | T [\Phi_D^a(x) \Phi_D^b(0)] | 0 \rangle = \delta^{ab} \frac{2}{3} J_P(W), \quad (23)$$

with $P^\mu = (W, 0, 0, 0)$. The loop functions for the ud and qs diquarks are obtained as

$$J_{ud}(W) = \frac{2}{3} J_P(W; M_q, M_q), \quad (24a)$$

$$J_{qs}(W) = \frac{2}{3} J_P(W; M_q, M_s), \quad (24b)$$

respectively.

The diquark mass is obtained as a pole position of the T matrix by solving Eq. (16). The calculated masses of the ud and qs scalar diquarks are plotted in the right panel of Fig. 1. Here we are interested in the flavor SU(3) breaking in the diquark masses, namely the mass difference between the ud and qs diquarks. The adjustment of their absolute values is out of the current scope. If one would need to reproduce diquark masses, one could tune the coefficient of the g_S term, which acts on the interaction kernels in a flavor symmetric way. The diquark masses are found above the qq and qs thresholds, and thus, the diquarks have a decay width. In the figure we show their real parts. We find that the mass difference of the diquark masses is insensitive to the G_k parameter. This means that the flavor SU(3) breaking in the diquark mass is still substantially large even for a finite G_k . Therefore, this suggest that the baryon masses could have a substantial flavor SU(3) breaking even if the constituent quark masses get degenerate.

4.2. Gell-Mann Oakes Renner relation

By introducing the anomaly induced interaction with the current quark mass into the model, the symmetry breaking pattern in this model is somewhat different from that in the original theory. The divergence of the axial vector current $A_\mu^a = \bar{\psi}\gamma_\mu\gamma_5\frac{\lambda^a}{2}\psi$ can be calculated by the Noether theorem:

$$\partial^\mu A_\mu^a = -i[\mathcal{L}_{\text{NJL}}, Q_A^a], \quad (25)$$

where Q_A^a is the generator of the axial transformation labeled by a . In the current model, the divergence of the third component of the axial vector current A_μ^3 is calculated as

$$\partial^\mu A_\mu^3 = m_q P^3 - g_k m_q (P^3 \bar{s}s + S^3 \bar{s}i\gamma_5 s - \bar{s}i\gamma_5 u \bar{u}s - \bar{u}i\gamma_5 s \bar{s}u + \bar{s}i\gamma_5 d \bar{d}s + \bar{d}i\gamma_5 d \bar{s}d), \quad (26)$$

where the pseudoscalar and scalar fields, P^a and S^a , are defined as $P^a = \bar{\psi}i\gamma_5\lambda^a\psi$ and $S^a = \bar{\psi}\lambda^a\psi$, respectively. This is the PCAC relation in this model and is different from that of QCD due to the presence of the g_k term.

The Gell-Mann Oakes Renner (GOR) relation [57] is derived by combining the Glashow Weinberg relation [58] and the PCAC relation. (See, for instance, Ref. [59].) The Glashow Weinberg relation is a relation in the chiral limit and reads for the massless pion

$$F_\pi G_\pi = -2\langle\bar{q}q\rangle, \quad (27)$$

with the matrix elements defined by

$$\langle 0|A_\mu^a(x)|\pi^b(p)\rangle = i\delta^{ab}p_\mu F_\pi e^{-ip\cdot x}, \quad (28)$$

$$\langle 0|P^a(x)|\pi^b(p)\rangle = \delta^{ab}G_\pi e^{-ip\cdot x}. \quad (29)$$

Taking the derivative of Eq. (28), we obtain, on one hand,

$$\langle 0|\partial^\mu A_\mu^a(x)|\pi^b(p)\rangle = \delta^{ab}m_\pi^2 F_\pi e^{-ip\cdot x}, \quad (30)$$

where the on-shell condition $p^2 = m_\pi^2$ is taken for pion. On the other hand, taking the matrix element for the vacuum and pion of the PCAC relation (26), we obtain

$$\langle 0|\partial^\mu A_\mu^3(x)|\pi^0(p)\rangle = m_q G_\pi (1 - g_k \langle\bar{s}s\rangle) e^{-ip\cdot x}, \quad (31)$$

for π^0 . Thus, from the PCAC relation we obtain

$$m_\pi^2 F_\pi = m_q G_\pi (1 - g_k \langle\bar{s}s\rangle). \quad (32)$$

Eliminating G_π from Eqs. (27) and (32), we obtain the Gell-Mann Oakes Renner relation for this model as

$$m_\pi^2 F_\pi^2 = -2m_q \langle \bar{q}q \rangle (1 - g_k \langle \bar{s}s \rangle). \quad (33)$$

Taking $g_k = 0$, one sees that the original form of the GOR relation is recovered. In the numerical calculations given in Sect. 3, the GOR relation (33) is satisfied with more than 99% precision, which is estimated by the ratio of the left hand side to the right hand side of Eq. (33) with the values obtained in our calculation.

Actually, Eq. (33) is consistent with the GOR relation in QCD. The current model is an effective model of QCD at low energy. According to the idea of the effective field theory, one presumes that the partition functions $Z[v, a, s, p]$ defined through the path integral form with external fields s, a, s, p should have common symmetry properties and should be shared by the original theory and the effective theory at low energy:

$$Z[v, a, s, p] = \int \mathcal{D}q \mathcal{D}\bar{q} \mathcal{D}G_\mu e^{i \int d^4x \mathcal{L}_{\text{QCD}}[v, a, s, p]} = \int \mathcal{D}\psi \mathcal{D}\bar{\psi} e^{i \int d^4x \mathcal{L}_{\text{NJL}}[v, a, s, p]}. \quad (34)$$

In this formulation, the quark condensate is obtained by

$$\langle \Omega | \bar{q}q | \Omega \rangle = -i \frac{1}{Z[0]} \left. \frac{\delta Z}{\delta s} \right|_{s=m_q, v=a=p=0}. \quad (35)$$

Calculating the above functional derivative for both theories in the mean field approximation, we obtain

$$\langle \bar{q}q \rangle_{\text{QCD}} = \langle \bar{q}q \rangle (1 - g_k \langle \bar{s}s \rangle), \quad (36)$$

where the left hand side denotes the quark condensate for QCD. This means that the mean fields in the current model may different from those in QCD. Combining Eqs. (33) and (36), one restores the original GOR relation for QCD. Equation (36) corresponds to Eq. (15) of Ref. [22] that was obtained in the linear sigma model.

5. Summary

We have investigated the scalar meson masses in the Nambu Jona-Lasinio model by solving the Bethe Salpeter equation for the quark-antiquark channels. Motivated by the previous work for the scalar meson masses in a linear σ model [22], we have introduced an axial anomaly induced interaction containing the current quark mass. Without this term, the $\bar{q}q$ scalar meson spectrum has an inconsistent ordering with observation that the κ meson with strangeness were heavier than the a_0 meson with isospin $I = 1$. The anomaly induced interaction with the current quark mass gives repulsion to the quark and antiquark systems for the flavor octet scalar channels, and it comes to the a_0 meson with a sizable strange current quark mass, while it does to the κ meson with a tiny up or down current quark mass. This different influence induces the reversal of the mass order between the a_0 and κ mesons. By fixing the model parameters to reproduce the masses of pion, kaon and the η' meson and the pion decay constant, we have calculated the scalar meson masses. We have found that around $G_k \simeq 1.0$ the masses of the a_0 and κ mesons get degenerate and for $G_k > 1.0$ the a_0 meson mass gets heavier than that of the κ meson. Thus, the inverse mass ordering is realized even in the $\bar{q}q$ configuration for the scalar meson. It is also interesting to mention that this model suggests that the constituent quark masses get degenerate for $G_k \simeq 2.0$. This might be inconsistent with the baryon mass spectra in which one sees substantial flavor SU(3)

breaking. By calculating the scalar diquark masses in the current model, we have found that the scalar diquark masses have still substantial flavor breaking even if the constituent quark masses get degenerate. Therefore, if the baryons have considerably large amount of the diquark component in their structure, the baryon masses still have enough flavor breaking even if the constituent quark masses get degenerate.

In conclusion, by introducing the U(1) axial anomaly term with the current quark mass, it is possible to realize the inverse mass ordering of the light scalar meson even in the $\bar{q}q$ picture. This fact would suggest that the $f_0(500)$ meson could be the chiral partner of the pion or at least should have a substantial component of the chiral partner.

Acknowledgements

The authors would like to thank Prof. Fujioka for his important suggestions. The work of D.J. was partly supported by Grants-in-Aid for Scientific Research from JSPS 21K03530. The work of M.H. is supported in part by JPSP KAKENHI Grant Number 20K03927.

A. Calculation details

In this appendix we show the calculation details of the formulae used in the NJL model. We perform the loop integrals with the three momentum cutoff Λ .

The quark condensate is calculated as

$$\langle \bar{\psi}\psi \rangle = -\frac{N_c M}{\pi^2} \int_0^\Lambda \frac{p^2}{\sqrt{p^2 + M^2}} dp = -\frac{N_c M \Lambda^2}{2\pi^2} \left(\sqrt{1 + \frac{M^2}{\Lambda^2}} - \frac{M^2}{\Lambda^2} \log \frac{\Lambda + \sqrt{\Lambda^2 + M^2}}{M} \right). \quad (\text{A1})$$

The loop functions for the scalar and pseudoscalar channels in the center of mass frame $P^\mu = (W, 0, 0, 0)$ are show for the energy below the threshold, $W \leq M_1 + M_2$, as

$$\begin{aligned} J_S(W; M_1, M_2) &= N_c i \int \frac{d^4 p}{(2\pi)^4} \text{Tr} \left[\frac{1}{\not{p} - M_1 + i\epsilon} \frac{1}{\not{p} - M_2 + i\epsilon} \right] \\ &= \frac{N_c \Lambda^2}{4\pi^2} \left\{ \sqrt{1 + \frac{M_1^2}{\Lambda^2}} - \frac{M_1^2 + M_2^2 - W^2}{2\Lambda^2} \log \frac{\Lambda + \sqrt{\Lambda^2 + M_1^2}}{M_1} \right. \\ &\quad - \frac{(M_1 + M_2)^2}{\Lambda^2} \frac{\omega_1}{W} \log \frac{\Lambda + \sqrt{\Lambda^2 + M_1^2}}{M_1} \\ &\quad \left. - \frac{W^2 - (M_1 + M_2)^2}{\Lambda^2} \frac{\eta}{W} \tan^{-1} \frac{\omega_1}{\eta} \sqrt{\frac{\Lambda^2}{\Lambda^2 + M_1^2}} \right\} + (M_1 \leftrightarrow M_2), \quad (\text{A2}) \end{aligned}$$

$$\begin{aligned} J_P(W; M_1, M_2) &= N_c i \int \frac{d^4 p}{(2\pi)^4} \text{Tr} \left[i\gamma_5 \frac{1}{\not{p} - M_1 + i\epsilon} i\gamma_5 \frac{1}{\not{p} - M_2 + i\epsilon} \right] \\ &= \frac{N_c \Lambda^2}{4\pi^2} \left\{ \sqrt{1 + \frac{M_1^2}{\Lambda^2}} - \frac{M_1^2 + M_2^2 - W^2}{2\Lambda^2} \log \frac{\Lambda + \sqrt{\Lambda^2 + M_1^2}}{M_1} \right. \\ &\quad - \frac{(M_1 - M_2)^2}{\Lambda^2} \frac{\omega_1}{W} \log \frac{\Lambda + \sqrt{\Lambda^2 + M_1^2}}{M_1} \\ &\quad \left. - \frac{W^2 - (M_1 - M_2)^2}{\Lambda^2} \frac{\eta}{W} \tan^{-1} \frac{\omega_1}{\eta} \sqrt{\frac{\Lambda^2}{\Lambda^2 + M_1^2}} \right\} + (M_1 \leftrightarrow M_2), \quad (\text{A3}) \end{aligned}$$

where we have defined

$$\omega_1 = \frac{W^2 + M_1^2 - M_2^2}{2W}, \quad \omega_2 = \frac{W^2 + M_2^2 - M_1^2}{2W}, \quad (\text{A4})$$

$$\eta = \frac{\sqrt{[(M_1 + M_2)^2 - W^2][W^2 - (M_1 - M_2)^2]}}{2\sqrt{s}}. \quad (\text{A5})$$

The analytic continuation from $W < M_1 + M_2$ to $W > M_1 + M_2$ can be performed as

$$\frac{\eta}{W} \tan^{-1} \frac{\omega_1}{\eta \sqrt{1 + M_1^2/\Lambda^2}} = \frac{q}{2W} \log \frac{q \sqrt{1 + \frac{M_1^2}{\Lambda^2}} + \omega_1}{q \sqrt{1 + \frac{M_1^2}{\Lambda^2}} - \omega_1}, \quad (\text{A6})$$

with

$$q = \frac{\sqrt{(W^2 - (M_1 + M_2)^2)(W^2 - (M_1 - M_2)^2)}}{2\sqrt{s}}. \quad (\text{A7})$$

The loop function with the axial current is calculated

$$\begin{aligned} J_A(W; M_1, M_2) &= N_c i \int \frac{d^4 p}{(2\pi)^4} \text{Tr} \left[\frac{\gamma^\mu \gamma_5}{2} \frac{1}{\not{p} - M_1 + i\epsilon} i\gamma_5 \frac{1}{\not{p} - \not{p} - M_2 + i\epsilon} \right] \\ &= -\frac{i N_c \Lambda}{4\pi^2} \left\{ \frac{\Lambda(M_2 - M_1)}{2W^2} \sqrt{1 + \frac{M_1^2}{\Lambda^2}} + \frac{M_1}{\Lambda} \frac{\omega_1}{W} \log \frac{\Lambda + \sqrt{\Lambda^2 + M_1^2}}{M_1} \right. \\ &\quad + \frac{M_1 - M_2}{\Lambda} \frac{\eta^2 - \omega_1^2}{2W^2} \log \frac{\Lambda + \sqrt{\Lambda^2 + M_1^2}}{M_1} \\ &\quad + \frac{M_1 + M_2}{\Lambda} \frac{(M_1 - M_2)^2 - W^2}{W^2} \frac{\eta}{2W} \tan^{-1} \frac{\omega_1}{\eta} \sqrt{\frac{\Lambda^2}{\Lambda^2 + M_1^2}} \left. \right\} \\ &\quad + (M_1 \leftrightarrow M_2). \end{aligned} \quad (\text{A8})$$

References

- [1] R.L. Workman *et al.* (Particle Data Group), Prog. Theor. Exp. Phys. 2022, 083C01 (2022).
- [2] R.L. Jaffe, Phys. Rev. **D15** 267 (1977).
- [3] M. Harada, F. Sannino and J. Schechter, Phys. Rev. D **54**, 1991-2004 (1996).
- [4] A. Dobado and J.R. Pelaez, Phys. Rev. **D56**, 3057 (1997).
- [5] J.A. Oller, E. Oset, and J.R. Pelaez, Phys. Rev. Lett. **80**, 3452 (1998).
- [6] J.A. Oller, E. Oset, and J.R. Pelaez, Phys. Rev. **D59**, 074001 (1999).
- [7] K. Igi and K. Hikasa, Phys. Rev. **D59**, 034005 (1999).
- [8] D. Black, A. H. Fariborz, F. Sannino and J. Schechter, Phys. Rev. D **59**, 074026 (1999)
- [9] M. Ishida, Prog. Theor. Phys. **101** (1999), 661-669.
- [10] T. Kunihiro *et al.* [SCALAR Collaboration], Phys. Rev. D **70**, 034504 (2004)
- [11] H. X. Chen, A. Hosaka and S. L. Zhu, Phys. Lett. B **650**, 369-372 (2007).
- [12] A. Zhang, T. Huang and T. G. Steele, Phys. Rev. D **76**, 036004 (2007).
- [13] M. R. Pennington, Mod. Phys. Lett. A **22**, 1439 (2007)
- [14] E. Klempt and A. Zaitsev, Phys. Rept. **454**, 1 (2007)
- [15] T. Kojo and D. Jido, Phys. Rev. D **78**, 114005 (2008).
- [16] A. H. Fariborz, R. Jora and J. Schechter, Phys. Rev. D **79**, 074014 (2009)
- [17] T. Hyodo, D. Jido, and T. Kunihiro, Nucl. Phys. **A848** (2010) 341.
- [18] D. Parganlija, P. Kovacs, G. Wolf, F. Giacosa and D. H. Rischke, Phys. Rev. D **87**, no. 1, 014011 (2013)
- [19] J. R. Peláez, Phys. Rept. **658**, 1 (2016)
- [20] J. R. Peláez, A. Rodas and J. Ruiz de Elvira, Eur. Phys. J. C **77**, no. 2, 91 (2017)
- [21] N. N. Achasov, Phys. Part. Nucl. **48**, no. 5, 681 (2017).
- [22] Y. Kuroda, M. Harada, S. Matsuzaki and D. Jido, Prog. Theo. Exp. Phys. **2020**, 053D02 (2020).
- [23] M. Gell-Mann and M. Levy, Nuovo Cim. **16** (1960) 705.

-
- [24] M. K. Volkov, *Annals Phys.* **157**, 282-303 (1984).
 - [25] S. Klimt, M. F. M. Lutz, U. Vogl and W. Weise, *Nucl. Phys. A* **516**, 429 (1990).
 - [26] U. Vogl, M. F. M. Lutz, S. Klimt and W. Weise, *Nucl. Phys. A* **516**, 469-495 (1990).
 - [27] V. Dmitrasinovic, *Nucl. Phys. A* **686**, 379-392 (2001).
 - [28] K. Naito, M. Oka, M. Takizawa and T. Umekawa *Prog. Theor. Phys.* **109**, 969 (2003)
 - [29] A. A. Osipov, H. Hansen and B. Hiller, *Nucl. Phys. A* **745**, 81-103 (2004).
 - [30] M. X. Su, L. Y. Xiao and H. Q. Zheng, *Nucl. Phys. A* **792**, 288-305 (2007).
 - [31] A.A. Osipov, B. Hiller, and A.H. Blin, *Eur. Phys. J.* **A49**, 14 (2013).
 - [32] A A. Osipov, B. Hiller, and A.H. Blin, *Phys. Rev.* **D88**, 054032 (2013).
 - [33] M. Kobayashi and T. Maskawa, *Prog. Theor. Phys.* **44** (1970) 1422. doi:10.1143/PTP.44.1422
 - [34] M. Kobayashi, H. Kondo and T. Maskawa, *Prog. Theor. Phys.* **45** (1971) 1955. doi:10.1143/PTP.45.1955
 - [35] J. Schechter, Y. Ueda, *Phys. Rev.* **D3** (1971) 168.
 - [36] G. 't Hooft, *Phys. Rev.* **D14** (1976) 3432.
 - [37] G. 't Hooft, *Phys. Rev. Lett.* **37** (1976) 8.
 - [38] C. Rosenzweig, J. Schechter and C. G. Trahern, *Phys. Rev. D* **21**, 3388 (1980).
 - [39] P. Di Vecchia and G. Veneziano, *Nucl. Phys. B* **171**, 253 (1980).
 - [40] E. Witten, *Annals Phys.* **128**, 363 (1980).
 - [41] K. Kawarabayashi, N. Ohta, *Nucl. Phys.* **B175** (1980) 477.
 - [42] Y. Nambu and G. Jona-Lasinio, *Phys. Rev.* **122** (1961) 345.
 - [43] V. Bernard, R. L. Jaffe and U. G. Meissner, *Phys. Lett. B* **198** (1987) 92.
 - [44] T. Kunihiro and T. Hatsuda, *Phys. Lett. B* **206** (1988) 385; Erratum: [*Phys. Lett. B* **210** (1988) 278].
 - [45] U. Vogl and W. Weise, *Prog. Part. Nucl. Phys.* **27** (1991) 195.
 - [46] T. Hatsuda and T. Kunihiro, *Phys. Rept.* **247** (1994) 221.
 - [47] S. Kono, D. Jido, Y. Kuroda and M. Harada, *PTEP* **2021** (2021) no.9, 093.
 - [48] M. Takizawa, Y. Nemoto and M. Oka, *Phys. Rev. D* **55** (1997), 4083.
 - [49] A. Buck, R. Alkofer, and H. Reinhardt, *Phys. Lett. B* **286** (1992) 29.
 - [50] N. Ishii, W. Bentz, and K. Yazaki, *Phys. Lett. B* **301** (1993) 165.
 - [51] N. Ishii, W. Bentz, and K. Yazaki, *Phys. Lett. B* **318** (1993) 26.
 - [52] N. Ishii, W. Bentz, and K. Yazaki, *Nucl. Phys.* **A587** (1995) 617.
 - [53] S. Huang and J. Tjon, *Phys. Rev. C* **49** (1994) 1702.
 - [54] U. Vogl, *Z. Phys.* **A337** (1990) 191.
 - [55] K. Suzuki and H. Toki, *Mod. Phys. Lett.* **A7** (1992) 2867.
 - [56] C. Weiss, A. Buck, R. Alkofer, and H. Reinhardt, *Phys. Lett. B* **312** (1993) 6.
 - [57] M. Gell-Mann, R.J. Oakes, and B. Renner, *Phys. Rev.* **175** (1968) 2195.
 - [58] S.L. Glashow, S. Weinberg, *Phys. Rev. Lett.* **20** 224 (1968).
 - [59] D. Jido, T. Hatsuda, and T. Kunihiro, *Phys. Lett.* **B670** (2008) 109.